A solar receiver with bubbling heat transfer for heating a pressurised gas

Conference Paper · December 2017

CITATIONS
0

READS
231

2 authors:

Mehdi Jafarian
University of Adelaide
42 PUBLICATIONS **538** CITATIONS
SEE PROFILE

Graham J Nathan
University of Adelaide
360 PUBLICATIONS **5,090** CITATIONS
SEE PROFILE

ASIA-PACIFIC SOLAR RESEARCH CONFERENCE

Peer Reviewed
2017 Solar Research Conference

Mehdi Jafarian

A solar receiver with bubbling heat transfer for heating a pressurised gas

Mehdi Jafarian and Graham J. Nathan

Centre for Energy Technology, Schools of Mechanical

The University of Adelaide, SA 5005, Australia

E-mail: mehdi.jafarian@adelaide.edu.au

Abstract

A novel solar receiver to indirectly heat a pressurised gas stream by bubbling it through a molten metal/metal oxide surrounding a cavity receiver is reported. The pressurised gas is injected as bubbles through the nozzles into the bath of heat transfer fluid, in which the cavity is suspended. This generates a high heat transfer rate to mitigate the exergy destruction that is typically associated with the indirect heating of a pressurised gas. The demonstration of a 1kW bench scale model of this receiver is reported using gallium and nitrogen as the heat transfer medium and working fluid, respectively. These experiments show that a low temperature difference can be achieved of approximately 10 °C between the temperature of the cavity and of the molten metal. In addition, the temperature difference between the molten metal bath and the outlet gas decreases as the gas flow rate increases. This implies that the heat transfer in this device is limited by the particular bubble configuration, so that even higher heat transfer rates are possible with optimisation of the bubbler.

1. Introduction

The solar to electrical efficiency of the concentrated solar power plants can be improved over current commercial technology through increasing the temperature of the inlet hot gas to the gas turbines (Kribus et al., 1998; Romero and Steinfeld, 2012). This has been demonstrated at pilot-scale using a hybrid solar gas turbine, in which the temperature of the pressurised air emerging from the solar receiver was further heated using combustion before its introduction to the gas turbine (Schwarzbözl et al., 2006). The target pressure in solar and solar-hybrid air Brayton cycles is in the range 3-35 bar, while the target temperature is around 1250 °C (Boyce, 2012). However, the upper end of these temperature and pressure ranges is yet to be demonstrated to operate reliably for extended periods due to the combined challenges resulting from the low thermal conductivity and heat capacity of air and the need to seal a pressurised receiver. That is, there is a fundamental incompatibility between the need for small gaps to achieve high heat transfer between a gas and a solid wall and the need for large clearance to avoid mechanical stresses from different thermal expansion. Therefore there is need to develop new solar receivers that offer the potential to achieve high heat transfer coefficients in pressurised devices that avoid generating high thermal stresses during heating or cooling.

Various configurations of the pressurised solar receivers have been proposed previously for both directly and indirectly heated concepts. In direct heating configurations, concentrated solar radiation (CSR) is either absorbed directly by the high pressure gas or by a surface (such as a particle), which is exposed to it. Outlet air temperatures of up to 1200 °C at a pressure of 20 bar with a peak efficiency of approximately 70% have been achieved in short-term trials (Buck et al., 2002; Karni et al., 1997; Pritzkow, 1991) using direct heating concepts (Hischier, 2011). However, to allow the fluid to be pressurised, these solar receivers require a transparent window which is vulnerable to high pressure, especially when the window size is increased to scales of more than 1 MW as is anticipated to be needed for industrial devices. It has been also shown that the application of a window imposes serious technical construction and operating problems owing to special requirements in optical properties, mechanical strength, high diurnal variable working temperature of the receiver, sealing, cooling and the need for a stress-less installation (Ávila-Marín, 2011; Posnansky and Pylkkänen, 1991; Pritzkow, 1991). Hence it is desirable to avoid the need for window.

In indirect heating concepts the working fluid is not directly exposed to either the CSR or the surface heated by it. In this method, CSR is first absorbed by radiation through a surface and then is transferred by conduction to a second surface, from which it is transferred to the pressurised air, mostly by convection. This avoids the need for the transparent window, but is achieved at the price of a lower heat transfer coefficient through the absorber walls and an associated lower outlet temperature (Jarvinen, 1977; Strumpf et al., 1982). The accompanying disadvantages are associated with the restrictions imposed by the material of the receiver wall, which requires resistance to thermal shock, good thermal conductivity and inertness to oxidation by air (Hischier, 2011). These introduce challenges to the structural integrity, since a high heat transfer coefficient typically leads to small clearances between the material surrounding the cavity and the cavity itself, which result in a high risk of thermal stresses being induced during heating and cooling. It is therefore desirable to identify alternative approaches that offer high rates of heat transfer together with low mechanical confinement to allow the cavity to expand or contract freely with no risk of contact with other components.

There are many industrial application in which a gas is bubbled through submerged injection ports into a liquid to promote the rate of heat and mass transfer between them (Deckwer, 1980; Leonard et al., 2015). These include the bottom blowing of oxygen into steel (Schwarz, 1996), the Pachuca tank used in the metallurgical industry and aerobic fermenters in biotechnologies (Chisti and Moo-Young, 1987; Shekhar and Evans, 1989). However, to the best knowledge of the authors, the potential advantages of bubbling media has yet to be investigated for solar receivers, with all receiver concepts explored to date being limited to either gas-only, liquid-only or particle based systems (Ho and Iverson, 2014; Piatkowski et al., 2011). The aim of the present investigation is therefore to explore the potential benefit of bubbling media to seek to mitigate the challenges of heating a pressurised fluid in a solar receiver. More specifically, we aim to directly assess its performance through a first-of-a-kind experimental investigations of a solar bubble receiver.

2. The solar bubble receiver

A novel and patent-pending indirectly heated solar receiver has been recently proposed at the University of Adelaide. This device employs a molten metal/metal oxide as the heat transfer

medium, to facilitate the heat transfer between the cavity and the pressurised gas (Jafarian et al., 2017). The key components of this solar receiver are shown in Figure 1. The CSR is absorbed by the inner surface of the cavity and transferred to the liquid bath through convection heat transfer from the outer surface of the cavity. The pressured gas is dispersed into the liquid bath from below the cavity to induce convective heat transfer between the bubbles, the bath and the surface.

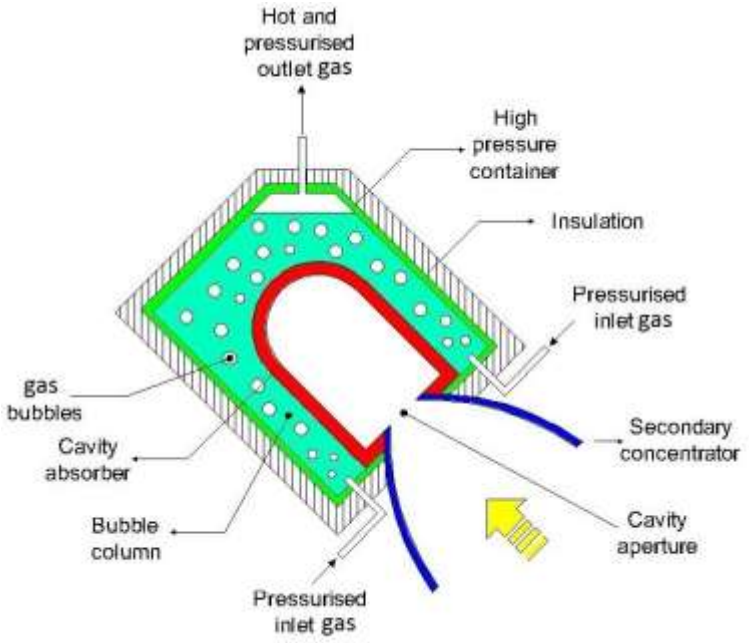

Figure 1. Schematic representation of the novel patent-pending high temperature solar cavity bubble receiver in a beam up configuration. The injected gas through the nozzles at the bottom of the molten metal/metal oxide column is heated by the concentrated solar radiation that is transferred through the cavity walls (Jafarian et al., 2017).

3. Methodology

3.1. Experimental arrangement and operative conditions

A schematic diagram of the bench-scale test-rig employed in this work is presented in Figure 2. The specific dimensions of the system are also shown. The system consists of a cavity that is submerged in a molten metal, here gallium (Ga), through which nitrogen (N_2) was injected as the heat transfer fluid. The inlet gas was injected into the molten bath through three nozzles, while the temperatures of the cavity, inlet and outlet gases were monitored using K-type thermocouples, shown as TC in Figures 2 and 3. The temperature distributions within the cavity wall in both r and ϕ directions were also monitored using K-type thermocouples, as shown in Figures 2 and 3. These were later used to measure the local heat transfer coefficient, $h_{\phi,cav,Ga}$, at the surface between the cavity and liquid gallium. A 1kW cartridge heater was employed to heat the cavity. Another thermocouple (shown as $TC_{C\text{-}H}$ in Figure 3) was also used to monitor the temperature of the cartridge heater. For the present experiments the temperature of the heater was set to 425 °C using a thermocouple (Figure 2) together with a temperature control

system (not shown). An array of 4 K-type thermocouples (Figure 2) were also used to monitor the temperature of the liquid Ga. Electronic mass flow controllers (ALICAT) were used to control the flow rates of N_2.

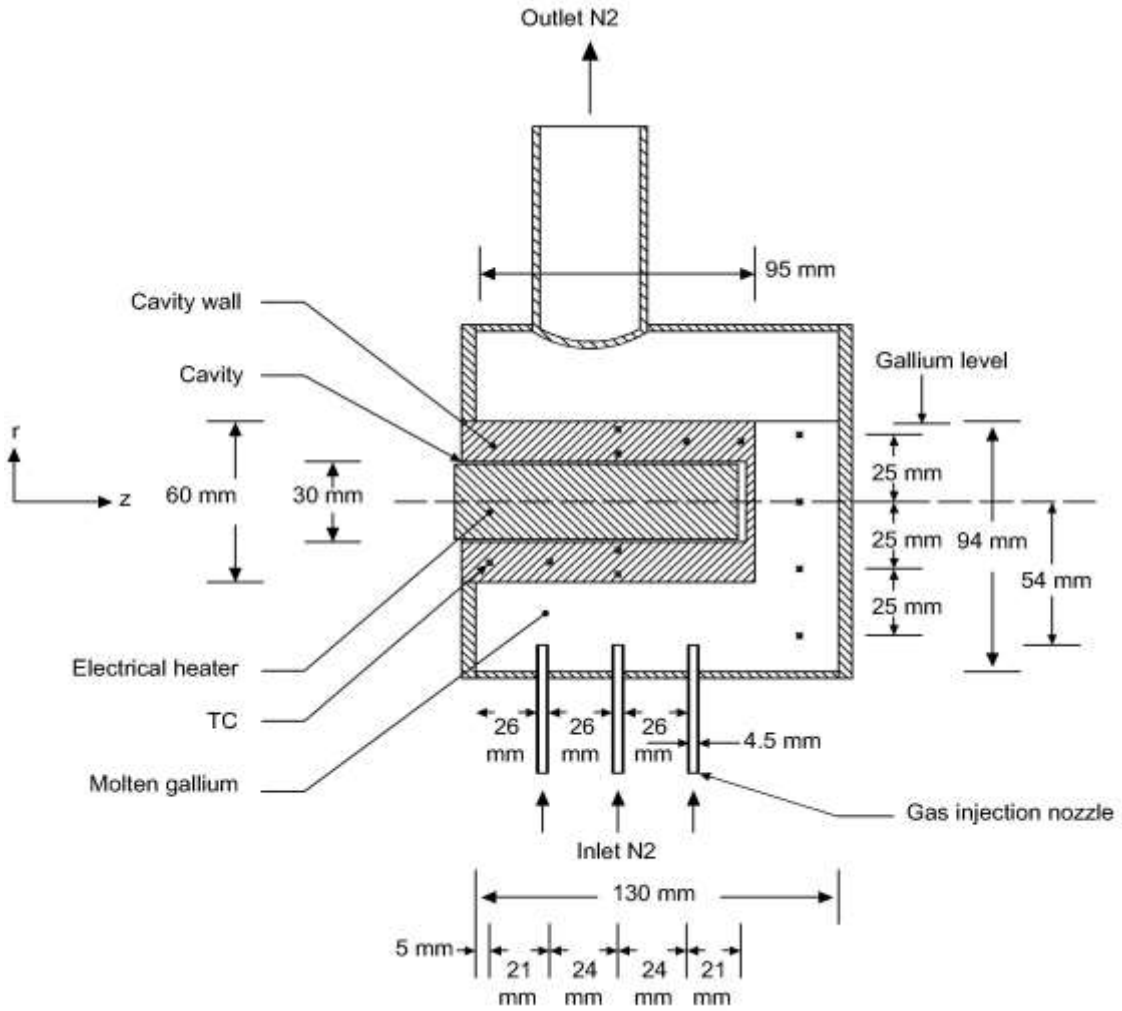

Figure 2. Schematic diagram of the 1-kW solar bubble receiver, with key dimensions and locations of the thermocouples.

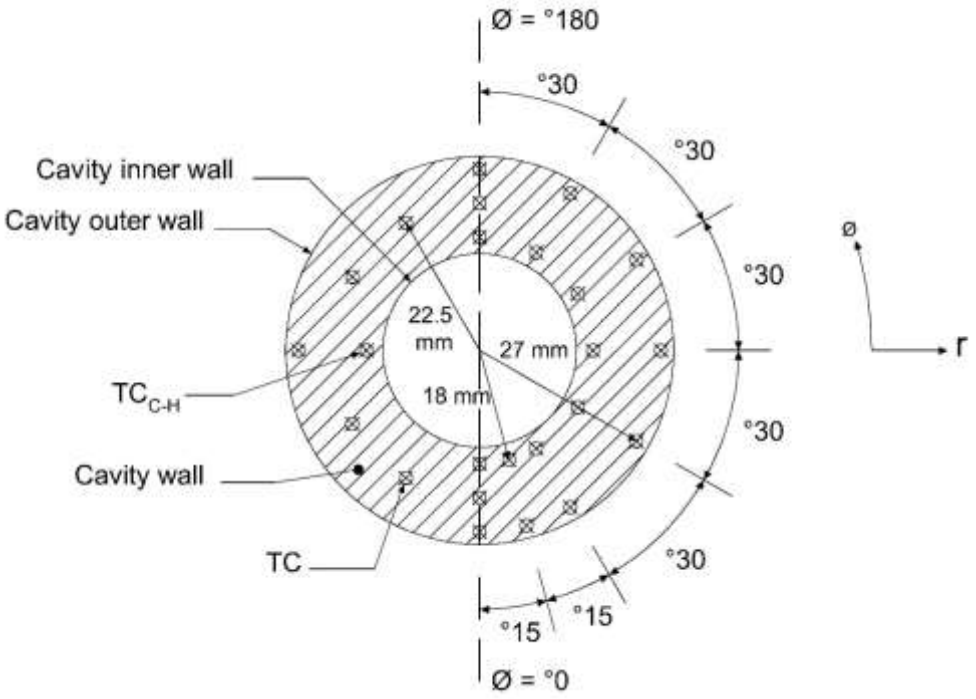

Figure 3. Schematic representation of the cavity and heater, showing the key dimensions and location of the thermocouples.

3.2. Heat transfer analysis

The local heat transfer coefficient between the cavity surface and molten gallium, $h_{\phi,cav,Ga}$, on the immersed cavity surface is given by:

$$h_{\phi,cav,Ga} = \frac{k\left.\frac{\partial T}{\partial r}\right|_{r=R_{out}}}{(T_{cav} - T_{Ga})}. \quad (1)$$

In this equation, R_{out} is the outer diameter of the cavity (Figure 3), T_{cav} is the surface temperature of the cavity, T_{Ga} is the average temperature of the liquid Ga and k is the thermal conductivity of the wall. The numerator of the Equation 1, represents the temperature gradient at the surface of the cavity. This was estimated from variations of temperature in r and ϕ directions at z = 41 mm only because the maximum temperature variation in temperature along the length of cavity (z direction) was approximately 10 °C. The point z = 41 mm is aligned with the center of the middle nozzle, as shown in Figure 2. The steady state temperature distribution inside the cavity wall in the r and ϕ directions is given by;

$$\left(\frac{\partial^2 T}{\partial r^2}\right) + \frac{1}{r}\left(\frac{\partial T}{\partial r}\right) + \frac{1}{r^2}\left(\frac{\partial^2 T}{\partial \phi^2}\right) = 0. \quad (2)$$

The boundary conditions required for the solution of Equation 2 are as follows:

$$T = T_{cav} \quad at \quad r = R_{in}\,, \tag{3}$$

$$T = T_{cav} \quad at \quad r = R_{out}\,, \tag{4}$$

$$T = T_{cav} \quad at \quad \phi = 0\,, \tag{5}$$

$$T = T_{cav} \quad at \quad \phi = \pi\,. \tag{6}$$

Here T_{cav} is the temperature of the cavity and R_{in} is the inner diameter of the cavity (Figure 3).

The average heat transfer coefficient at the cavity surface between the cavity surface and molten Ga, $\bar{h}_{cav,Ga}$, is given by:

$$\bar{h}_{cav,Ga} = \frac{1}{A_{out,cav}} \int_{A_{out,cav}} h_{\varphi,cav,Ga}\, dA\,. \tag{7}$$

In this equation $A_{out,cav}$ is the outlet surface of the cavity.

The Reynolds number of the outlet gas from the injection nozzles is defined as:

$$\mathrm{Re}_N = \frac{\rho_g v_g D_N}{\mu}\,, \tag{8}$$

where ρ_g, μ and are the density, viscosity and velocity of the outlet gas from the nozzles, while D_N is the nozzle diameter. The mean average temperature of the cavity wall, $T_{m,cav}$, and molten Ga, $T_{m,Ga}$, are also reported.

4. Results and discussion

Figure 4 presents the measured temperature of the outlet N_2, mean average temperature of the cavity surface, $T_{m,cav}$, and the average temperature of the molten liquid, $T_{m,Ga}$, as a function of Reynolds number of the outlet N_2 from the injection nozzles, Re_N. It can be seen that while there is only a small difference of approximately 10 °C between the $T_{m,cav}$ and $T_{m,Ga}$ in all assessed range of Re_N, the difference between the temperature of the outlet N_2 and that of the molten Ga decreases significantly from 260 °C at Re_N = 1600 to 52 °C at Re_N = 12800. Furthermore the effect of Re_N on outlet N_2 temperature is more significant at low values of Re_N than high ones. For example, an increase in Re_N from 1600 to 3200 drops the temperature difference between the outlet N_2 and molten Ga by 28%, while this drop is approximately 18% for increasing of Re_N from 11200 to 12800. This indicates that the rate of heat transfer between the N_2 and molten Ga, depends strongly on the turbulence induced within the gas-liquid system by injection of gas, while the rate of heat transfer between the liquid Ga and hot surface is almost independent from it.

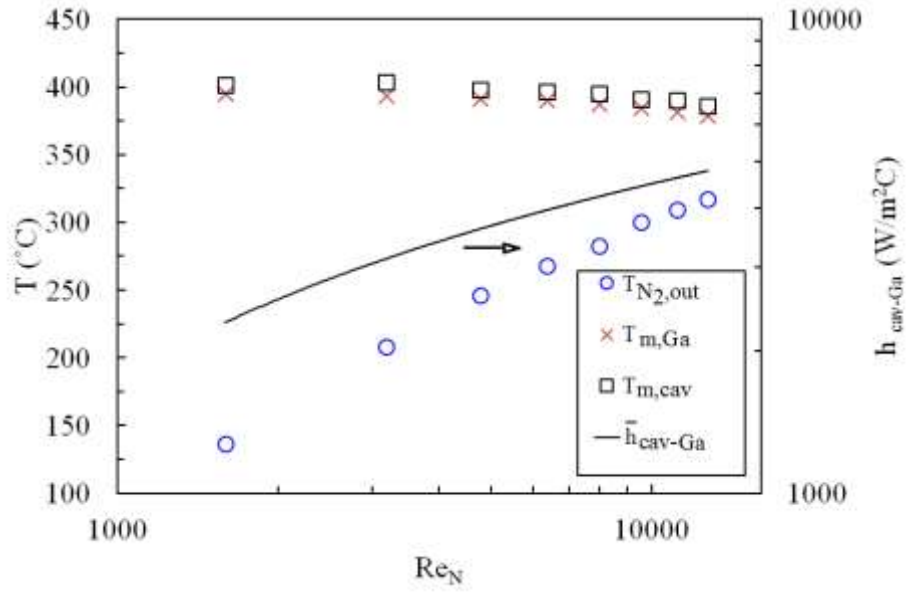

Figure 4. Measured temperature of the outlet N_2, mean temperature of the molten gallium and mean temperature of the cavity surface (left hand axis) together with the estimated average heat transfer coefficient on cavity surface between the cavity surface and the molten gallium (right hand axis).

Figure 5 presents the measured distribution of the local heat transfer on the cavity surface, $h_{\phi,cav,Ga}$, as a function of azimuthal angle, ϕ, for different Re_N. As can be seen $h_{\varphi,cav,Ga}$ was found to depend significantly on ϕ. In particular, in the assessed range of Re_N the maximum $h_{\varphi,cav,Ga}$ was found to occur, at $\phi < 20°$ and $\phi = 180°$, together with another peak at $\phi \sim 60°$ for the higher Reynolds number cases. The peaks at $\phi < 20°$ and 180 ° can be attributed to the forward and rear stagnation points at the surface of a cylinder, while the $\phi \sim 60°$ case is probably attributed to combined influences of flow separation around the cylinder and the role of buoyancy, although further work is needed to assess this better. It can be also seen that a local minimum in $h_{\phi,cav,Ga}$ is found at $\phi = °150$. It was also found that $h_{\phi,cav,Ga}$ on the cavity surface increases relatively with Re_N in all assessed range of Re_N. This is in agreement with the variations of the average heat transfer coefficient on cavity surface, $\bar{h}_{cav,Ga}$, with Re_N, shown in Figure 4. It can be seen that $\bar{h}_{cav,Ga}$ increases significantly from 2600 W/m^{2}C at Re_N = 1600 to 4900 W/m^{2}C at Re_N = 12800. This demonstrates the significance of the flow regime around the cavity on the heat transfer coefficient, which depends significantly on the nozzle designs in term of size and location within the cavity.

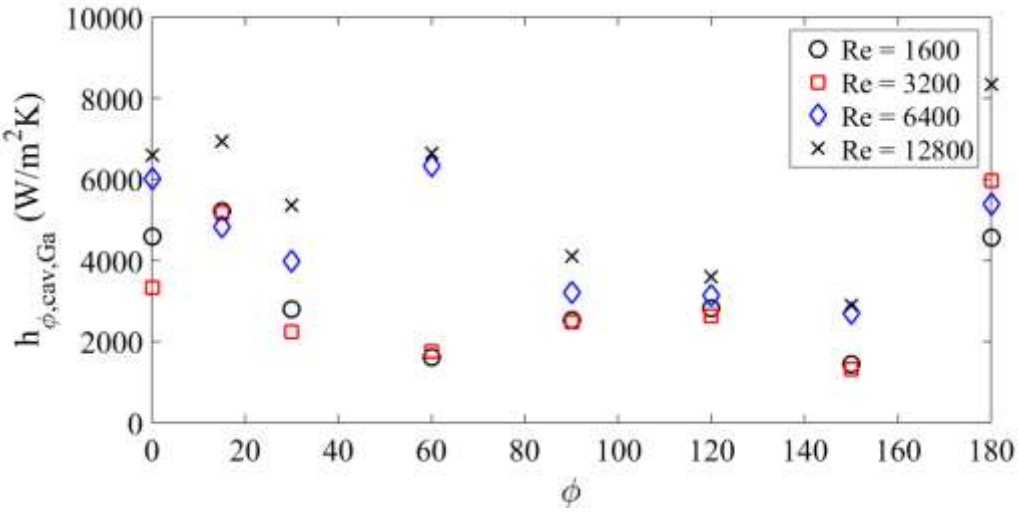

Figure 5. Variations of local heat transfer coefficient with azimuthal position in the cavity surface for different nozzles Reynolds number.

5. Conclusions

These small scale trials demonstrate that there is good potential to achieve high rates of heat transfer between a gas and a cavity receiver by bubbling it through a molten metal. Good heat transfer coefficients were measured, with a temperature difference of only 10 °C between the temperature of the cavity and that of the molten metal. In addition, the temperature difference between the molten metal bath and the outlet gas decreases as the gas flow rate is increased, which implies even higher heat transfer rates are possible with optimization of the bubbler. Nevertheless, it is premature to conclude strong potential for industrial-scale solar thermal receivers, since the effects of scale are not yet well understood.

The specific outcomes from the experimental investigation on the concept of using a bubbling gas within a liquid metal as heat transfer medium in a small-scale solar receiver are as follows:

- The temperature difference between the molten gallium and cavity surface is almost independent of Re_N, while the temperature of the outlet gas is strongly sensitive to it.
- The local heat transfer between the cavity and Ga, $h_{\phi,cav,Ga}$ varies significantly with φ in 1600 <Re_N < 12800. The maximum $h_{\phi,cav,Ga}$ is achieved at φ = °0 and ϕ = °180, while the minimum of $h_{\phi,cav,Ga}$ has occurred at φ = °150.

References

Ávila-Marín, A.L., 2011. Volumetric receivers in solar thermal power plants with central receiver system technology: a review. Solar Energy 85, 891-910.
Boyce, M.P., 2012. Gas turbine engineering handbook. Butterworth-Heinemann.
Buck, R., Brauning, T., Denk, T., Pfander, M., Schwarzbozl, P., Tellez, F., 2002. Solar-hybrid gas turbine-based power tower systems (REFOS). Journal of Solar Energy Engineering 124, 2-9.

Chisti, M.Y., Moo-Young, M., 1987. Airlift reactors: characteristics, applications and design considerations. Chemical Engineering Communications 60, 195-242.
Deckwer, W.D., 1980. On the mechanism of heat transfer in bubble column reactors. Chemical Engineering Science 35, 1341-1346.
Hischier, I., 2011. Developement of a pressurized receiver for solar-driven gas turbine. ETH ZURICH.
Ho, C.K., Iverson, B.D., 2014. Review of high-temperature central receiver designs for concentrating solar power. Renewable and Sustainable Energy Reviews 29, 835-846.
Jafarian, M., Abdollahi, M.R., Nathan, G.J., 2017. Solar receiver, provisional patent application. australian provisional patent application 2017900564, Adelaide Research and Innovation, Australia, Priority date: 21 Feb 2017.
Jarvinen, P.O., 1977. Solar-heated-air receivers. Solar Energy 19, 139-147.
Karni, J., Rubin, R., Sagie, D., Fiterman, A., Kribus, A., Doron, P., 1997. The DIAPR: A high-pressure, high-temperature solar receiver. Journal of Solar Energy Engineering 119, 74-78.
Kribus, A., Zaibel, R., Carey, D., Segal, A., Karni, J., 1998. A solar-driven combined cycle power plant. Solar Energy 62, 121-129.
Leonard, C., Ferrasse, J.H., Boutin, O., Lefevre, S., Viand, A., 2015. Bubble column reactors for high pressures and high temperatures operation. Chemical Engineering Research and Design 100, 391-421.
Piatkowski, N., Wieckert, C., Weimer, A.W., Steinfeld, A., 2011. Solar-driven gasification of carbonaceous feedstock-a review. Energy & Environmental Science 4, 73-82.
Posnansky, M., Pylkkänen, T., 1991. Development and testing of a volumetric gas receiver for high-temperature applications. Solar Energy Materials 24, 204-209.
Pritzkow, W.E.C., 1991. Pressure loaded volumetric ceramic receiver. Solar Energy Materials 24, 498-507.
Romero, M., Steinfeld, A., 2012. Concentrating solar thermal power and thermochemical fuels. Energy & Environmental Science 5, 9234-9245.
Schwarz, M.P., 1996. Simulation of gas injection into liquid melts. Applied Mathematical Modelling 20, 41-51.
Schwarzbözl, P., Buck, R., Sugarmen, C., Ring, A., Marcos Crespo, M.J., Altwegg, P., Enrile, J., 2006. Solar gas turbine systems: Design, cost and perspectives. Solar Energy 80, 1231-1240.
Shekhar, R., Evans, J.W., 1989. Fluid flow in pachuca (air-agitated) tanks: Part I. Laboratory-scale experimental measurements. Metallurgical and Materials Transactions B 20, 781-791.
Strumpf, H.J., Kotchick, D.M., Coombs, M.G., 1982. High-temperature ceramic heat exchanger element for a solar thermal receiver. Journal of Solar Energy Engineering 104, 305-309.

Acknowledgements

This research was performed as part of the Australian Solar Thermal Research Initiative (ASTRI), a project supported by the Australian Government, through the Australian Renewable Energy Agency (ARENA), ARENA 1-SRI002. This program has been also supported by the Australian Research Council (ARC) through grant DP150102230. The views expressed herein are not necessarily the views of the Australian Government, and the Australian Government does not accept responsibility for any information or advice contained herein.